WHITE DWARFS AND THE AGE OF THE UNIVERSE

JORDI ISERN
Institut d'Estudis Espacials de Catalunya, E-08034 Barcelona, SPAIN
Institut de Ciències de l'Espai (Consejo Superior de Investigaciones Científicas), E-08034 Barcelona, SPAIN
ENRIQUE GARCIA–BERRO
Institut d'Estudis Espacials de Catalunya, E-08034 Barcelona, SPAIN
Departament de Física Aplicada, Escola Politècnica Superior de Castelldefels, Universitat Politècnica de Catalunya, E-08860 Castelldefels, SPAIN

Abstract: White dwarfs are the final remnants of low and intermediate mass stars. Their evolution is essentially a cooling process that lasts for ~ 10 Gyr and allows to obtain information about the age of the Galaxy as well as about the past stellar formation rate in the solar neighborhood. One of the most important applications is to pose a severe constrain to the age of the Universe. For this reason it is important to identify all the relevant sources of energy as well as the mechanisms that control its flow to the space. In this paper we describe the state of the art of the white dwarf cooling theory and we discuss the uncertainties still remaining.

1 Introduction

The test of self-consistency that all the cosmological models have to fullfill is that the Universe cannot by younger than anyone of the objects it contains. For this reason a huge effort has been invested to identify and determine the age of the oldest objects in the Universe: globular clusters and long-lived stars. In this contribution we examine the role that white dwarfs can play in this affair.

White dwarfs represent the last evolutionary stage of stars with masses smaller than $10 \pm 2\ M_{\odot}$, with the upper mass limit not yet well known. Most of them are composed of carbon and oxygen, but white dwarfs with masses smaller than $0.4\ M_{\odot}$ are made of helium, while those more massive than $\sim 1.05\ M_{\odot}$ are made of oxygen and neon. The exact composition of the carbon-oxygen cores critically depends on the evolution during the previous asymptotic giant branch phase, and more specifically on the competition between the $^{12}\mathrm{C}(\alpha,\gamma)^{16}\mathrm{O}$ reaction and the triple-α reaction, on the details of the stellar evolutionary codes and on the choice of several other nuclear

cross sections. In a typical case, a white dwarf of 0.58 $M_\odot$, the total amount of oxygen represents the 62% of the total mass while its concentration in the central layers of the white dwarf can be as high as 85%.

In all cases, the core is surrounded by a thin layer of pure helium with a mass in the range of 10^{-2} to 10^{-4} $M_\odot$. This layer is, in turn, surrounded by an even thinner layer of hydrogen with mass lying in the range of 10^{-4} to 10^{-15} $M_\odot$. This layer is missing in 25% of the cases. From the phenomenological point of view, white dwarfs containing hydrogen are classified as DA while the remaining ones (the non-DA) are classified as DO, DB, DQ, DZ and DC, depending on their spectral features, and constitute a sequence of decreasing temperatures. The origin of these spectral differences and the relationship among them is not yet elucidated although it is related to the initial conditions imposed by the evolution of AGB stars, the diffusion induced by gravity, thermal diffusion, radiative levitation, convection at the H-He and He-core interfaces, proton burning, stellar winds and mass accretion from the interstellar medium.

The structure of white dwarfs is sustained by the pressure of degenerate electrons and these stars cannot obtain energy from thermonuclear reactions. Therefore, their evolution can be described just as a simple cooling process [1] in which the internal degenerate core acts as a reservoir of energy and the outer non-degenerate layers control the energy outflow. If it is assumed that the core is isothermal, which is justified by the high conductivity of degenerate electrons, and that the envelope is thin, then

$$L \approx -\frac{dU_{\rm th}}{dt} = -\overline{c_{\rm V}} M_{\rm WD} \frac{dT_{\rm c}}{dt} \tag{1}$$

where $U_{\rm th}$ is the thermal content, $\overline{c_{\rm V}}$ is the average specific heat, $T_{\rm c}$ is the temperature of the (isothermal) core and all the remaining symbols have their usual meaning. To solve this equation it is necessary to provide a relationship among the luminosity and the temperature of the core:

$$\frac{L}{M_{\rm WD}} = f(T_{\rm c}) \tag{2}$$

A simple calculation indicates that the lifetime of these stars is very long, ~ 10 Gyr, and thus they retain important information about the past history of the Galaxy. In particular, it is possible to obtain the stellar formation rate and the age of the different galactic components: disk, halo and globular clusters.

2 The evolution of the envelope

As it has been mentioned earlier, the envelope of white dwarf stars is a very thin layer ($M_{\rm e} < 10^{-2}$ $M_\odot$), partially degenerate, partially or totally ionized and sometimes

convective, that completely controls the emergent flux of energy. Its behavior is the result of:

1. A non–standard initial chemical composition resulting from hydrogen and helium shell burning in AGB stars,

2. A very efficient gravitational settling that induces the stratification of the envelope in almost chemically pure layers with the lightest element in the top [2], and

3. The existence of mechanisms tending to restore the homogeneity, like convective mixing [3, 4, 5, 6], radiative levitation [7, 8], thermal diffusion [2], accretion from the interstellar medium [9], winds and so on.

There is now a broad opinion that the distinction among the character DA and non–DA is inherited (i.e., it is linked to the origin of the white dwarf itself) although a fraction of them can change their external aspect during the evolution [10]. Standard evolution theory predicts that typical field white dwarfs have a core mass in the range of 0.5 to 1.0 $M_\odot$ made of a mixture of carbon and oxygen surrounded by a helium mantle of $M_{\rm He} \simeq 10^{-2} M_{\rm WD}$, surrounded itself by a hydrogen envelope of $M_{\rm H} \simeq 10^{-4} M_{\rm WD}$ [3, 11, 12]. Adjusting the parameters in the AGB models it is possible to obtain in the 25% of the cases a white dwarf totally devoid of the hydrogen layer. Since the relative number of DA/non–DA stars changes as the evolution proceeds, a mechanism able to change this property must exist [10, 13].

The idea is that DA white dwarfs start as a central star of a planetary nebula. When its temperature is high enough ($T_{\rm eff} > 40,000$ K) radiative levitation brings metals to the photosphere and heavy element lines appear in its spectrum. As the temperature goes down, these elements settle down and disappear. When DAs arrive to the instability strip they pulsate as ZZ Ceti stars. Pulsational data indicates that the masses of the hydrogen layer are in the range between 10^{-8} and $10^{-4}\, M_\odot$ thus indicating that DAs are born with a variety of layer masses. As the DA star cools down, the convective region deepens and, depending on the mass, reaches the helium layer. When this happens, helium is dredged up and the DA white dwarf turns into a non–DA. Consequently, the ratio between the number of DAs and non–DAs decreases. Stars with a thin H layer ($< 10^{-9}\ M_\odot$) mix at high temperatures while those having a thick layer ($\sim 10^{-4}\ M_\odot$) never do it.

The evolution of a non–DA star is more complex. They are born as He-rich central stars of planetary nebulae and, as they cool down, they become first PG 1159 stars and then DO stars. The trace amounts of hydrogen still present in the helium envelope gradually float up to the surface and when the effective temperature is of the order of 50,000 K the outer H layer becomes thick enough to hide the He layer and to convert the star into a DA star. When the temperature drops below 30,000 K,

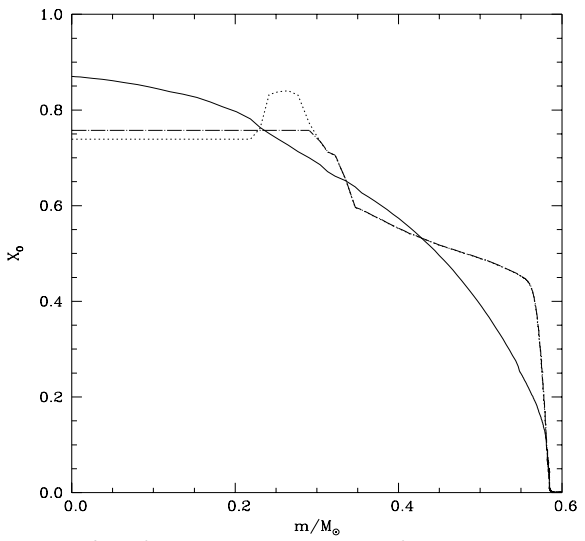

Figure 1: Oxygen profile of a 0.61 $M_\odot$ white dwarf at the beginning of the thermally-pulsing AGB phase (dotted line), the same after rehomogenization by Rayleigh-Taylor instabilities during the liquid phase (dotted-dashed line) and after total freezing (solid line).

the helium convection zone increases and hydrogen is engulfed and mixed within the helium layer once more. The white dwarf is observed as a non–DA, more precisely as a DB. This lack of non–DA stars in the temperature range of 30,000 to 45,000 K is known as the DB gap. The DB stars gradually cool down and become DZ and DC stars (a fraction of them being DAs in origin). Due to the convective dredge up at the bottom of the helium envelope, some of the non–DAs show carbon in their spectra (DQ stars). Because of accretion from the interstellar medium some of them show hydrogen lines in their spectrum (they are known as DBA class).

3 Overview of white dwarf evolution

The evolution of white dwarfs from the planetary nebula phase to its disappearance depends on the properties of the envelope and the core and has been discussed in detail [11, 12, 14, 15, 16]. To summarize, the cooling process can be roughly divided in four stages: neutrino cooling, fluid cooling, crystallization and Debye cooling.

- *Neutrino cooling:* $\log(L/L_\odot) > -1.5$. This stage is very complicated because of the dependence on the initial conditions of the star as well as on the complex and not yet well understood behavior of the envelope. For instance, it

has been found that the luminosity due to hydrogen burning through the pp chains would never stop and could even become dominant at low luminosities, $-3.5 \leq \log(L/L_\odot) \leq -1.5$. It is worth noting that, if this were the case, the cooling rate would be similar to the normal one (i.e., the one that neglects this source) and it would be observationally impossible to distinguish between both possibilities. However, the importance of such a source strongly depends on the mass, $M_{\rm H}$, of the hydrogen layer. If $M_{\rm H} \leq 10^{-4}\ M_\odot$, the pp contribution quickly drops and never becomes dominant. Since astero-seismological observations seem to constrain the size of $M_{\rm H}$ well below this critical value, this source can be neglected. Fortunately, when neutrino emission becomes dominant, the different thermal structures converge to a unique one, making sure the uniformity of the models with $\log(L/L_\odot) \lesssim -1.5$. Furthermore, since the time necessary to reach this value is $\lesssim 8 \times 10^7$ years for any model, its influence in the total cooling time is negligible.

- *Fluid cooling:* $-1.5 \geq \log(L/L_\odot) \geq -3$ The main source of energy is the gravothermal one. Since the plasma is not very strongly coupled ($\Gamma < 179$), its properties are reasonably well known. Furthermore, the flux of energy through the envelope is controlled by a thick nondegenerate layer with an opacity dominated by hydrogen (if present) and helium, and weakly dependent on the metal content. The main source of uncertainty is related to the chemical structure of the interior, which depends on the adopted rate of the $^{12}{\rm C}(\alpha,\gamma)^{16}{\rm O}$ reaction and on the treatement given to semiconvection and overshooting. If this rate is high, the oxygen abundance is higher in the center than in the outer layers, resulting thus in a reduction of the specific heat at the central layers where the oxygen abundance can reach values as high as $X_{\rm O} = 0.85$ [17].

- *crystallization:* $\log(L/L_\odot) < -3$. Crystallization introduces two new sources of energy: latent heat and sedimentation. In the case of Coulomb plasmas, the latent heat is small, of the order of $k_{\rm B}T_{\rm s}$ per nuclei, where $k_{\rm B}$ is the Boltzmann constant and $T_{\rm s}$ is the temperature of solidification. Its contribution to the total luminosity is between ~ 5 and 10% [18].

During the crystallization process, the equilibrium chemical compositions of the solid and liquid plasmas are not equal. Therefore, if the resulting solid is denser than the liquid mixture, it sink towards the central region. If they are lighter, they rise upwards and melt when the solidification temperature, which depends on the density, becomes equal to that of the isothermal core. The net effect is a migration of the heavier elements towards the central regions with the subsequent release of gravitational energy [19]. Of course, the efficiency of the process depends on the detailed chemical composition and on the initial chemical profile and it is maximum for a mixture made of half oxygen and half

carbon uniformly distributed through all the star.

- *Debye cooling:* When almost all the star has solidified, the specific heat follows the Debye's law. However, the outer layers still have very large temperatures as compared with the Debye's one, and since their total heat capacity is still large enough, they prevent the sudden disappearance of the white dwarf in the case, at least, of thick envelopes.

Figure 1 displays the oxygen profiles for the CO core of a $\sim 0.6\ M_\odot$ white dwarf progenitor obtained just at the end of the first thermal pulse (dotted line). The inner part of the core, with a constant abundance of ^{16}O, is determined by the maximum extension of the central He-burning convective region while the peak in the oxygen abundance is produced when the He-burning shell crosses the semiconvective region partially enriched in ^{12}C and ^{16}O, and carbon is converted into oxygen through the $^{12}\mathrm{C}(\alpha,\gamma)^{16}\mathrm{O}$ reaction. Beyond this region, the oxygen profile is built when the thick He-burning shell is moving towards the surface. Simultaneously, gravitational contraction increases its temperature and density, and since the ratio between the $^{12}\mathrm{C}(\alpha,\gamma)^{16}\mathrm{O}$ and 3α reaction rates is lower for larger temperatures the oxygen mass fraction steadily decreases in the external part of the CO core.

The ^{12}C and ^{16}O profiles at the end of the first thermal pulse have an off-centered peak in the oxygen profile, which is related to semiconvection. Since [17] chosed the rate of [20] for the $^{12}\mathrm{C}(\alpha,\gamma)^{16}\mathrm{O}$ reaction, they were forced to use the Scwarzschild criterion for convection and, therefore, they did not find the chemical profiles to be Rayleigh-Taylor unstable during the early thermally-pulsing AGB phase. After the ejection of the envelope, when the nuclear reactions are negligible at the edge of the degenerate core, the Ledoux criterion can be used and, therefore, the chemical profiles are Rayleigh-Taylor unstable and, consequently, are rehomogeneized by convection. Notice that, in any case, this rehomogeneization minimizes the effect of the separation occurring during the cooling process. Figure 1 also shows the resulting oxygen profile after rehomogeneization (dotted-dashed line), and the oxygen profile after complete crystallization (solid line).

4 The physics of the cooling

The local energy budget of the white dwarf can be written as:

$$\frac{dL_{\rm r}}{dm} = -\epsilon_\nu - P\frac{dV}{dt} - \frac{dE}{dt} \tag{3}$$

where all the symbols have their usual meaning. If the white dwarf is made of two chemical species with atomic numbers Z_0 and Z_1, mass numbers A_0 and A_1, and

abundances by mass X_0 and X_1, respectively ($X_0 + X_1 = 1$), where the suffix 0 refers to the heavier component, this equation can be written as:

$$\begin{aligned} -(\frac{dL_{\rm r}}{dm} + \epsilon_\nu) &= C_{\rm v}\frac{dT}{dt} + T\Big(\frac{\partial P}{\partial T}\Big)_{V,X_0}\frac{dV}{dt} \\ &\quad -l_{\rm s}\frac{dM_{\rm s}}{dt}\delta(m - M_{\rm s}) + \\ &\quad \Big(\frac{\partial E}{\partial X_0}\Big)_{T,V}\frac{X_0}{dt} \end{aligned} \tag{4}$$

where $l_{\rm s}$ is the latent heat of crystallization and $\dot{M}_{\rm s}$ is the rate at which the solid core grows; the delta function indicates that the latent heat is released at the solidification front. Notice that chemical differentiation contributes to the luminosity not only through compressional work, which is negligible, but also through the change in the chemical abundances, which leads to the last term of this equation. Notice, as well, that the largest contribution to $L_{\rm r}$ due to the change in E exactly cancels out the $P\,dV$ work for *any* evolutionary change (with or without a compositional change). This is, of course, a well known result [1, 18, 21, 22] that can be related to the release of gravitational energy [23].

Integrating over the whole star, we obtain:

$$\begin{aligned} L + L_\nu &= -\int_0^{M_{\rm WD}} C_{\rm v}\frac{dT}{dt}\,dm \\ &\quad -\int_0^{M_{\rm WD}} T\Big(\frac{\partial P}{\partial T}\Big)_{V,X_0}\frac{dV}{dt}\,dm \\ &\quad + \ l_{\rm s}\frac{dM_{\rm s}}{dt} \\ &\quad -\int_0^{M_{\rm WD}} \Big(\frac{\partial E}{\partial X_0}\Big)_{T,V}\frac{dX_0}{dt}\,dm \end{aligned} \tag{5}$$

The first term of the equation is the well known contribution of the heat capacity of the star to the total luminosity [1]. The second term represents the contribution to the luminosity due to the change of volume. It is in general small since only the thermal part of the electronic pressure, the ideal part of the ions and the Coulomb terms other than the Madelung term contribute [18, 21]. However, when the white dwarf enters into the Debye regime, this term provides about the 80% of the total luminosity preventing the sudden disappearence of the star [22]. The third term represents the contribution of the latent heat to the total luminosity at freezing. The fourth term represents the energy released by the chemical readjustement of the white dwarf, i.e., the release of the energy stored in the form of chemical potentials. This term is usually negligible in normal stars, since it is much smaller than the energy

Mixture	ΔE (erg)	Δt (Gyr)
C/O	1.95×10^{46}	1.81
A/Ne	1.52×10^{47}	9.09
A/Fe	2.00×10^{46}	1.09
C/O/Ne	0.20×10^{46}	0.60

Table 1: Energy released by the chemical differentiation induced by crystallization and the corresponding delays.

released by nuclear reactions, but it must be taken into account when all other energy sources are small.

The last term can be further expanded and written as [23]:

$$\int_0^{M_{\rm WD}} \left(\frac{\partial E}{\partial X_0}\right)_{T,V} \frac{dX_0}{dt}\, dm = (X_0^{\rm sol} - X_0^{\rm liq}) \left[\left(\frac{\partial E}{\partial X_0}\right)_{M_{\rm s}} - \left\langle \frac{\partial E}{\partial X_0} \right\rangle\right] \frac{dM_{\rm s}}{dt} \tag{6}$$

where

$$\left\langle \frac{\partial E}{\partial X_0} \right\rangle = \frac{1}{\Delta M} \int_{\Delta M} \left(\frac{\partial E}{\partial X_0}\right)_{T,V} dm \tag{7}$$

and it is possible to define the total energy released per gram of crystallized matter as:

$$\epsilon_{\rm g} = -(X_0^{\rm sol} - X_0^{\rm liq}) \left[\left(\frac{\partial E}{\partial X_0}\right)_{M_{\rm s}} - \left\langle \frac{\partial E}{\partial X_0} \right\rangle\right] \tag{8}$$

The square bracket is negative since $(\partial E/\partial X_0)$ is negative and essentially depends on the density, which monotonically decreases outwards.

The contribution of any source or sink of energy to the cooling rate can be easily computed. For instance, the delay introduced by solidification can be easily estimated to a good approximation if it is assumed that the luminosity of the white dwarf is just a function of the temperature of the nearly isothermal core [23]. In this case:

$$\Delta t = \int_0^{M_{\rm WD}} \frac{\epsilon_{\rm g}(T_{\rm c})}{L(T_{\rm c})}\, dm \tag{9}$$

where $\epsilon_{\rm g}$ is is the energy released per unit of crystallized mass and $T_{\rm c}$ is the temperature of the core when the crystallization front is located at m. Of course, the

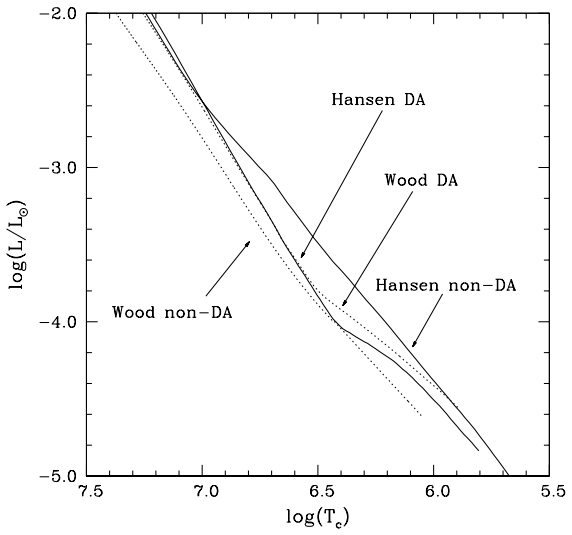

Figure 2: The relationships between the core temperature and the luminosity for various model atmospheres, see text for details.

total delay essentially depends on the transparency of the envelope. Any change in one sense or another can amplify or damp the influence of solidification and for the moment there are not reliable envelope models at low luminosities.

Table 4 displays the energy released in a, otherwise typical, 0.6 $M_{\odot}$ white dwarf and the delays introduced by the different cases of solidification discussed here assuming that the envelope is the same as in [23] and [15] and that the white dwarf is made of half carbon and half oxygen. The symbol A represents the effective binary mixture. Its use is probably justified in the case of impurities of very high number such as iron. However, in the case of Ne this assumption is most probably doubtful.

As previously stated, the total delay depends on the transparency of the envelope. In order to illustrate the effects of the transparency of the envelope in the cooling times, in Figure 2 we show several different core temperature–luminosity relationships. The first model atmosphere was obtained from the DA model sequence of [24], which has a mass fraction of the helium layer of $q_{\rm He} = 10^{-4}$ and a hydrogen layer of $q_{\rm H} = 10^{-2}$; the second model atmosphere is the non-DA model sequence [25] which has a helium layer of $q_{\rm He} = 10^{-4}$. However it should be noted that between these two model sequences there was a substantial change in the opacities, and therefore the comparison is meaningless (i.e., the non-DA model is more opaque than the DA one). The remaining two model atmospheres are those of [26] for both DA and non-DA white dwarfs. These atmospheres have been computed with state of the art physical inputs for both the equation of state and the opacities for the range of densities and

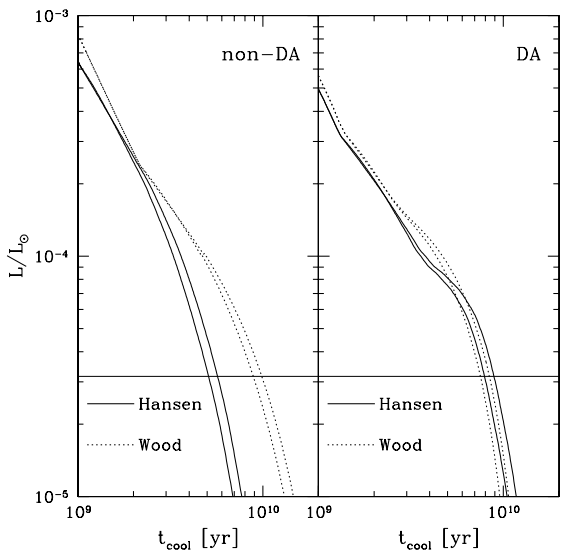

Figure 3: Cooling curves (time is in yr) for the white dwarf models described in the text, the thinner horizontal line corresponds to $\log(L/L_\odot) = -4.5$, which is the approximate position of the observed cut-off of the white dwarf luminosity function.

temperatures relevant for white dwarf envelopes (although it should be mentioned that the contributions to the opacity of H^{3+} and H^{2+} ions were neglected in this calculation) and have the same hydrogen and helium layer mass fractions as those of [24] and [25], respectively. In all the cases, the mass of the white dwarf is 0.606 $M_\odot$ and the initial chemical profile of the C/O mixture is that of [17].

From Figure 2 one can clearly see that the DA model atmospheres of [24] and [26] are in very good agreement down to temperatures of the order of $\log(T_c) \simeq 6.5$, whereas at lower temperatures the model atmospheres of [26] predict significantly lower luminosities (that is, they are less transparent). In contrast, the non-DA model atmosphere of [26] is by far more transparent at any temperature than the corresponding model of [25]. This is clearly due to the fact that this model was based on the old Los Alamos opacities and include a finite contribution from metals whereas the non-DA atmospheres of [26] are made of pure helium.

With these two sets of model atmospheres [27] computed cooling sequences for the following two cases: 1) crystallization and no phase separation and 2) crystallization and phase separation. The results are shown in Figure 3. The left panel of this figure shows the cooling sequences for the non-DA model envelopes of Hansen — solid lines — and Wood & Winget — dotted lines. The sequences with phase separation correspond, obviously, to the cooling curves with larger cooling times for the same luminosity. The right panel of the figure shows the same set of calculations for the

Input	Δt (Gyr)	Comments
DA/non–DA	$\lesssim 3.0$	Very uncertain
Core composition	$\lesssim 0.5$	Depending on the $^{12}C(\alpha,\gamma)^{16}O$
Opacity	$\lesssim 0.4$	
Metals in the envelope	≈ 0.2	
Additive contributions of the crystallization process		
C/O	0.8–1.2	Depending on the $^{12}C(\alpha,\gamma)^{16}O$
Fe	$\lesssim 1.3$	
Ne	$\lesssim 9.0$	Binary mixture
	$\lesssim 0.5$	Ternary mixture
Observational	1–2	

Table 2: Uncertainties in the estimates of the cooling time of white dwarfs.

hydrogen-dominated white dwarf envelopes described previously. Clearly the cooling times are very different depending on the assumed physical characteristics of the adopted atmosphere.

Table 4 displays the uncertainties in the time necessary to fade until $\log(L/L_\odot) = -4.5$. In the lower section of this table the additive contributions to the uncertainty due to the physics of crystallization are shown, whereas the upper section describes the uncertainties due to the rest of the input physics. As it can be seen, the major contribution is provided by the minor chemical species.

On the other hand, it is worth noticing at this point that white dwarfs provide the unique oportunity to check their cooling process in nearly real time. In particular, it is of interest to note that among white dwarfs there is a specific class of stars, known as ZZ-Ceti objects, which have a hydrogen-rich envelope (thus being classified as DA white dwarfs) and show periodic variations in their light curves. G117-B15A belongs to this particular set of stars. The observed periods of pulsation are 215.2, 271 and 304.4 s together with harmonics and linear combinations of the quoted periods, being the dominant pulsation mode the 215.2 s mode. The luminosity variations have been successfully explained as due to g-mode pulsations. G117-B15A has been recently claimed to be the most stable optical clock ever found, being the rate of change of the 215.2 s period very small: $\dot{P} = (2.3 \pm 1.4) \times 10^{-15}\,\mathrm{s\,s^{-1}}$, with a stability comparable to that of the most stable millisecond pulsars [28]. The rate of change of the period is closely related to its cooling timescale, which can be accurately computed, thus offering a unique opportunity to test any additional (or hypothetical) sink of energy.

$$\frac{d\ln P}{dt} \propto -\frac{d\ln T}{dt} \propto \frac{1}{\tau_{\rm cool}} \tag{10}$$

We have looked for a model that matches the three observed modes as good

as possible [29]. The model that provides the best fit to the observations is $M_\star = 0.55\,M_\odot$,$l = 1$, $k = 2, 3, 4$ and $\log M_{\rm H}/M_\star = -4.0$. The rate of change of the period for this model is $\dot{P} = 3.9\times10^{-15}{\rm s\,s^{-1}}$. Therefore, the agreement between observations and theory is better than a factor of two. After examining all the possible uncertainties a few words are necessary to justify the discrepancy between this value and the measured rate of change of the period of the 215.2 s mode, $\dot{P} = (2.3\pm1.4)\times10^{-15}{\rm s\,s^{-1}}$, and its computed value for the fiducial model. First, the theoretical uncertainties performed in this work can account for a spread of about $\pm1\times10^{-15}{\rm s\,s^{-1}}$. Second, the parallax and proper motion [28, 30] contribute as much as $\dot{P} = (9.2\pm0.5)\times10^{-16}{\rm s\,s^{-1}}$. We thus conclude that taking into account all this uncertainties our preferred model could be safely considered as satisfactory and that our value for $\dot{P}$ is fully consistent with the observed rate of change of the period.

5 The age and the properties of the Galactic disk and halo

The white dwarf luminosity function is defined as the number of white dwarfs with bolometric magnitude $M_{\rm bol}$ per cubic parsec and unit bolometric magnitude. The first luminosity functions were obtained by [31]. Since then it has been largely improved [32, 33, 34, 35, 36]. The two main properties of this empirical luminosity function are its monotonic increase when the luminosity decreases, which indicates the cooling nature of the evolution of white dwarfs, and the existence of a short fall at $\log(L/L_\odot) \approx -4.5$ which is interpreted as a consequence of the finite age of the Galaxy. From the comparison between this empirical function and the theoretical one, it is possible to obtain the age of the disk, T, and the star formation rate, $\Psi(t)$, as a function of time [37, 38, 39, 40, 41].

Regarding the luminosity function of halo white dwarfs very few things can be said due to the lack of observational data. However there have been considerable efforts to improve the actual situation [42, 43]. Hopefully, future missions like GAIA will remedy this situation [44].

The luminosity function can be computed as

$$n(l) \propto \int_{M_{\rm i}}^{M_{\rm s}} \Phi(M)\,\Psi(T - t_{\rm cool}(l, M) - t_{\rm MS}(M))\tau_{\rm cool}(l, M)\,dM \qquad (11)$$

where l is the logarithm of the luminosity in solar units, M is the mass of the parent star (for convenience all white dwarfs are labelled with the mass of the main sequence progenitor), $t_{\rm cool}$ is the cooling time down to luminosity l, $\tau_{\rm cool} = dt/dM_{\rm bol}$ is the characteristic cooling time, $M_{\rm s}$ and $M_{\rm i}$ are the maximum and the minimum masses of the main sequence stars able to produce a white dwarf of luminosity l, $t_{\rm MS}$ is the main sequence lifetime of the progenitor of the white dwarf, and T is the age

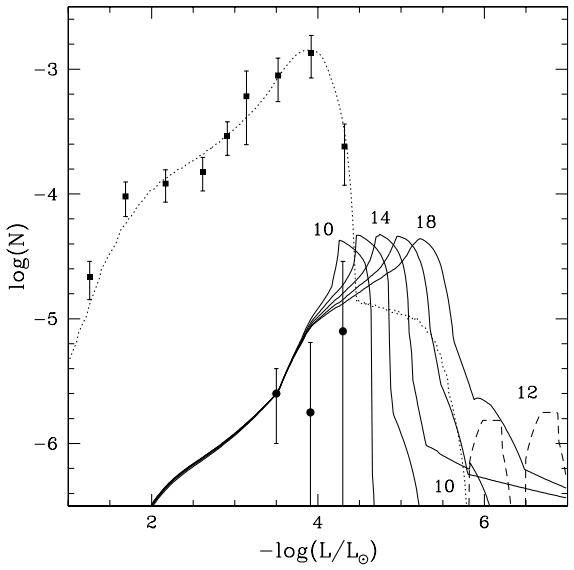

Figure 4: Luminosity functions of disk and halo white dwarfs as a function of the luminosity.

of the population under study. The remaining quantities, the initial mass function, $\Phi(M)$, and the star formation rate, $\Psi(t)$, are not known a priori and depend on the astronomical properties of the stellar population under study.

In order to compare with the observations properly, it is convenient to bin this function in intervals of magnitude $\Delta M_{\rm bol}$, usually one or half magnitudes, in the following way:

$$\langle n(l)\rangle_{\Delta l} = \frac{1}{\Delta l}\int_{l-0.5\Delta l}^{l+0.5\Delta l} n(l)\; dl \tag{12}$$

where Δl is the size of the luminosity bin that corresponds to $\Delta M_{\rm bol}$. It is important to notice here that this binning procedure smooths and ultimately erases the spikes introduced by the sedimentation of Ne and Fe in the observational luminosity function. Therefore, in order to observationally detect the influence of these impurities it would be necessary to have high resolution luminosity functions.

Figure 4 displays the luminosity functions of halo and disk white dwarfs computed with the standard initial mass function. The adopted cooling sequences were those of those from [17], which do not include the effects of Ne and Fe. The theoretical luminosity functions were normalized to the points $\log(L/L_\odot) \simeq -3.5$ and $\log(L/L_\odot) \simeq -2.9$ for the halo and the disk respectively due to their smaller error bars [45]. The luminosity function of the disk was obtained assuming an age of the

disk of 9.2 Gyr and a constant star formation rate per unit volume for the disk, and those of the halo assuming a burst that lasted 0.1 Gyr and started at $t_{\rm halo}$= 10, 12, 14, 16 and 18 Gyr respectively. Due to their higher cooling rate, O–Ne white dwarfs produce a long tail in the disk luminosity function and a bump (only shown in the cases $t_{\rm halo}$= 10 and 12 Gyr) in the halo luminosity function. The detection of such peaks should allow the determination of the age of the galactic halo.

During the derivation of the age of the disk it has been assumed that the star formation rate per unit volume has remained constant all the time along the life of our Galaxy. However, some models of galactic evolution predict that the process of formation of stars started in the central regions of the Galaxy and propagated outwards. If this was the case, a gradual instead of a prompt increase of the star formation rate would be expected. As it can be seen from the definition of the luminosity function, it is impossible to separate the age of the Galaxy from the star formation rate because of the extremely long lifetimes of low mass main sequence stars. That is, very old low mass main sequence stars are able to produce young (in the sense of cooling times) and bright white dwarfs. This implies that the past star formation activity is still influencing the present white dwarf birthrate. This property offers the unique opportunity to obtain the true age of the solar neighborhood instead of just providing a lower limit [41].

The star formation rate can be obtained by solving the inverse problem posed by the definition of the luminosity function. However, since the kernel of the transformation is not symmetric and has a complicated behavior [41], it is not possible to obtain a direct solution and its unicity cannot be guaranteed. Therefore, the only procedure consists in the adoption of a trial function as a star formation rate. This trial function depends on a set of $\mathbf{p}$ parameters, and we search for the values of these parameters that best fit the observed luminosity function. That is, we minimize the following function:

$$f(\mathbf{p}) = \sum_{i=1}^{n} \Big[\frac{\phi_i(\mathbf{p}) - \Phi_{\rm i}(l_{\rm i})}{\delta\Phi_{\rm i}} \Big]^2 \tag{13}$$

where $\phi_{\rm i}(\mathbf{p})$ and $\Phi_{\rm i}$ are the computed and the observed values of the luminosity function, respectively, and $\delta\Phi_{\rm i}$ are the corresponding error bars of each bin.

As trial functions we have chosen the following three cases:

1. A constant star formation rate, Ψ;
2. An almost constant star formation rate plus a relatively extended tail:

$$\Psi(t) \propto \frac{1}{1 + {\rm e}^{(t-\tau)/\delta}};$$

and,

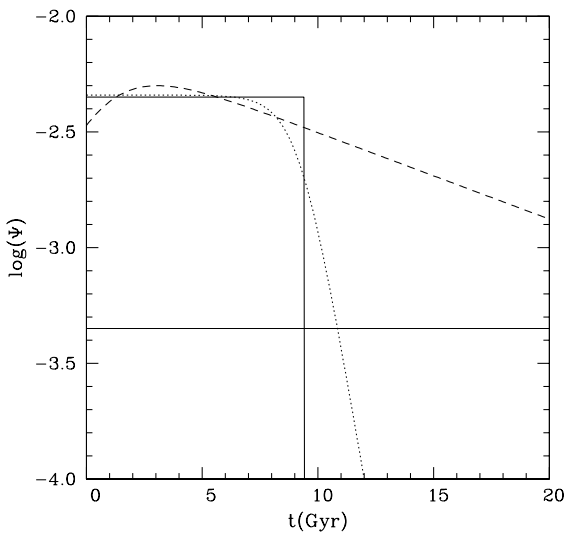

Figure 5: Star formation rates that provide a good fit to the observed luminosity function. The horizontal line correspond to 1/10 of the present star formation rate. The units of Ψ are ($M_\odot$ pc^{-3} Gyr^{-1}).

3. A star formation rate per unit surface that decreases with a timescale $\tau_{\rm s}$, divided by an scale height above the galactic plane that decreases with a timescale $\tau_{\rm h}$:

$$\Psi(t) \propto \frac{{\rm e}^{-t/\tau_{\rm s}}}{1 + A\,{\rm e}^{-t/\tau_{\rm h}}}.$$

As it is obvious the fits are better when more parameters are considered [41].

Figure 5 displays the star formation rates obtained by solving the inverse problem. It is clear that this function has remained nearly constant, within a factor 2, during the last 9–12 Gyr and that this behavior is compatible with a previous epoch, that could have lasted 2–8 Gyr, of lower activity before reaching the present values. The age of the solar neighborhood obtained in cases 1, 2 and 3 are 9.5, 11 and 20 Gyr respectively.

It is important to notice that since the bright side of the luminosity function is insensitive to the shape of the star formation rate [45], there is a degeneracy in the set of solutions to equation 1. This degeneracy can be removed by improving the dim branch, by obtaining the luminosity of massive white dwarfs and combining these data with statistical properties of red dwarfs.

6 Conclusions

White dwarf are well studied objects and the physical processes that control their evolution are relatively well understood. In fact most phases of white dwarf evolution can be succesfully characterized as a cooling process. That is, white dwarfs slowly radiate at the expense of their residual grovothermal energy. This release of energy lasts for long time scales (of the order of the age of the galactic disk: 10^{10} yr). While their detailed energy budget is still today the subject of some debate, their mechanical structures, which are largely supported by the pressure of the gas of degenerate electrons, are very well modeled except for the outer layers. These layers control the output of energy and a correct modeling is necessary to understand the evolution of white dwarfs.

The sedimentation of chemical species induced by crystallization is a major source of energy of coolest white dwarf stars. The delay introduced by the C/O partial separation is of the order of 1 Gyr (this quantity depends on the model of atmosphere adopted). Minor species present in the white dwarf can also introduce huge delays that can range from 0.5 to 9 Gyr. This uncertainty will be solved when good ternary phase diagrams are available.

White dwarfs can provide important information about the age of the galactic disk by comparing their luminosity function at low luminosities, and specially the position of its cut-off, with the theoretical predictions. For this purpose it is necessary to have good theoretical models and good observational data. From the observational point of view, the main sources of uncertainty are the distance to the lowest luminosity white dwarfs, the bolometric corrections, and the chemical composition of the outer layers (i.e., DA if hydrogen is present non-DA if hydrogen is absent). Nowadays, the contribution of the observational uncertainties to the total error budget of the galactic age can be estimated to be as large as 2 Gyr. Of this amount, 1 Gyr comes directly from the binning and sampling procedure and the statistical noise of the low luminosity bins [46].

From the observational point of view, the obtention of good luminosity functions of the disk or globular clusters with resolutions in magnitude better than 0.5 magnitudes could easily allow to test the different phase diagrams. Furthermore, an accurate luminosity function of disk white dwarfs can not only provide a tight constrain to the galactic age and to the shape of the phase diagram of binary mixtures but also has the bonus of providing important information about the temporal variation of the star formation rate.

The scarcity of bright halo white dwarfs and the lack of the good kinematical data necessary to distinguish halo white dwarfs from those of the disk have prevented up to now the construction of a good luminosity function for the halo [43] but probably future missions like GAIA will completely change the situation since high–quality parallaxes and proper motions will result in accurate tangential velocities, thus allowing

a good discrimination of these two populations.

Theoretical models indicate that if the halo is not too old, about 12 Gyr, there would be a reasonable chance to detect the corresponding cut off ($M_V \sim 16$) with surveys as deep as $m_V \sim 20$, provided that the DA specimen were dominant. On the contrary, if non-DA white dwarfs turn out to be dominant, the cut-off would be placed at absolute magnitudes as large as 20 and there would be no chance to detect it and, thus to constrain in this way the age of the halo. In any case, indirect information about the halo (age, duration of the burst,...) will come from the comparison of the absolute numbers of red halo dwarfs and white dwarfs in a complete volume limited sample. Furthermore, a robust determination of the bright part of the halo luminosity function could provide important information on the allowed IMFs for the halo and decisively contribute to the solution of the problems posed by the gravitational lensing observations in our halo. Therefore, a simultaneous and self-consistent determination of photometric properties, parallaxes and proper motions of halo white dwarfs could provide us with an unique opportunity to set up a solid platform for the study of the halo properties and to set up constraints to its dark matter content.

Acknowledgements: This work has been partially supported by the MCyT grants AYA04094–C03–01 and 02, by the European Union FEDER funds, and by the CIRIT.

References

[1] Mestel, L. 1952, MNRAS, 112, 583
[2] Schatzman, E. 1958, *White Dwarfs*, (Amsterdam: North–Holland)
[3] D'Antona, F., Mazzitelli, I. 1978, A&A, 66, 453
[4] Fontaine, G., Villeneuve, B., Wesemael, F., Wegner, G. 1984, ApJ, 227, L61
[5] Pelletier, C., Fontaine, G., Wesemael, F., Michaud, G., Wegner, G. 1986, ApJ, 307, 242
[6] MacDonald, J., Hernanz, M., José, J. 1998, MNRAS, 296, 523
[7] Fontaine, G., Michaud, G. 1979, ApJ, 231, 826
[8] Vauclair, G., Vauclair, S., Greenstein, J. 1979, A&A, 80, 79
[9] Alcock, C., Illarionov, A. 1980, ApJ, 235, 534
[10] Shipman, H. 1997, in *White Dwarfs*, Ed.: J. Isern, M. Hernanz, E. García–Berro (Dordrecht: Kluwer), p. 165
[11] Iben, I., Tutukov, A. V. 1984, ApJ, 282, 615
[12] Koester, D., Schönberner, D. 1986, A&A, 154, 125
[13] Fontaine, G., Wesemael, F. 1997, in *White Dwarfs*, Ed.: J. Isern, M. Hernanz, E. García–Berro (Dordrecht: Kluwer), p. 173
[14] D'Antona, F., Mazzitelli, I. 1989, ApJ, 347, 934
[15] Ségretain, L., Chabrier, G., Hernanz, M., García–Berro, E., Isern, J., Mochkovitch, R. 1994, ApJ, 434, 641

[16] Isern, J., García–Berro, E., Hernanz, M., Mochkovitch, R. 1998, J. Phys.: Condens. Matter, 10, 11263
[17] Salaris, M., Domínguez, I., García–Berro, E., Hernanz, M., Isern, J., Mochkovitch, R. 1997, ApJ, 486, 413
[18] Shaviv, G., Kovetz, A. 1976, A&A, 51, 383
[19] Mochkovitch, R. 1983, A&A, 122, 212
[20] Caughlan, G.R., Fowler, W.A., Harris, M.J., Zimmermann, B.A. 1985, *Atomic Data and Nuclear Data Tables*, 32, 197
[21] Lamb, D.Q., Van Horn, H.M. 1975, ApJ, 200, 306
[22] D'Antona, F., Mazzitelli, I. 1990, ARA&A, 28, 139
[23] Isern, J., Mochkovitch, R., García–Berro, E., Hernanz, M. 1997, ApJ, 485, 308
[24] Wood, M.A., in *White Dwarfs*, eds. Koester, D., Werner, K. 1995, (Berlin: Springer), p. 41
[25] Wood, M.A., Winget, D.E. 1989, in IAU Colloq. 114, *White Dwarfs*, ed. Wegner, G. (Berlin: Springer), p. 282
[26] Hansen, B.M.S. 1999, ApJ, 520, 680
[27] Isern, J.., García–Berro, E., Hernanz, M., Chabrier, G. 2000, ApJ, 528, 397
[28] Kepler, S.O., Mukadam, A., Winget, D.E., Nather,R.E., Metcalfe, T.S., Reed, M.D., Kawaler, S.D., Bradley, P.A. 2000, ApJ, 534, L185
[29] Córsico, A.H., Benvenuto, O.G., Altahus, L.G., Isern, J., García–Berro, E. 2001, New Astronomy, 6, 197
[30] Pajdosz, G. 1995, A&A, 295, L17
[31] Weidemann, V. 1968, ARA&A, 6, 351
[32] Fleming, T.A. , Liebert, J., Green, R.F. 1986, ApJ, 308, 176
[33] Liebert, J., Dahn, C.C., Monet, D.G. 1988, ApJ, 332, 891
[34] Oswalt, T.D., Smith, J.A., Wood, M.A., Hintzen, P. 1996, Nature, 382, 692
[35] Leggett, S.K., Ruiz, M.T., Bergeron, P. 1998, ApJ, 497, 294
[36] Knox, R.A., Hawkins, M.R.S., Hambly, N.C. 1999, MNRAS, 306, 736
[37] García–Berro, E., Hernanz, M., Isern, J., Mochkovitch, R. 1988, A&A, 193, 141
[38] Yuan, J.W. 1989, A&A, 224, 108
[39] Hernanz, M., García–Berro, E., Isern, J., Mochkovitch, R., Ségretain, L., Chabrier, G. 1994, ApJ, 434, 652
[40] Díaz–Pinto, A., García–Berro, E., Hernanz, M., Isern, J., Mochkovitch, R. 1994, A&A, 282, 86
[41] Isern, J., García–Berro, E., Hernanz, M., Mochkovitch, R., Burkert, A. 1995, in *"White Dwarfs"*, ed. Koester, D., Werner, K., Lecture Notes in Physics, 443 (Berlin: Springer), p. 19
[42] Liebert, J., Dahn, C.C., Monet, D.G. 1989, in *"White Dwarfs"*, Eds.: Wegner, G., *IAU Coll. 114*, (Berlin: Springer), p. 15
[43] Torres, S. , García–Berro, E., Isern, J. 1998, ApJ, 508, L71
[44] Figueras, F., García–Berro, E., Torra, J., Jordi, C., Luri, X., Torres S., Chen, B. 1999, Balt. Astron., 8, 291

[45] Isern, J., García–Berro, E., Hernanz, M., Mochkovitch, R., Torres, S. 1998, ApJ, 503, 239
[46] García–Berro, E., Torres, S., Isern, J., Burkert, A. 1999, MNRAS, 303, 173